JACS
JOURNAL OF THE AMERICAN CHEMICAL SOCIETY
Article
Cite This: J. Am. Chem. Soc. XXXX, XXX, XXX−XXX
pubs.acs.org/JACS

Tris-*N*-Nitrilotriacetic Acid Fluorophore as a Self-Healing Dye for Single-Molecule Fluorescence Imaging

Viktorija Glembockyte,[†,§] Ralph Wieneke,[‡] Karl Gatterdam,[‡] Yasser Gidi,[†] Robert Tampé,*[,‡] and Gonzalo Cosa*[,†]

[†]Department of Chemistry and Quebec Centre for Applied Materials (QCAM), McGill University, 801 Sherbrooke Street W., H3A 0B8 Montreal, Quebec, Canada

[‡]Institute of Biochemistry, Biocenter, and Cluster of Excellence − Macromolecular Complexes, Goethe University Frankfurt, Max-von-Laue-Str. 9, 60438 Frankfurt/M., Germany

Supporting Information

ABSTRACT: The photostability of fluorescent labels comprises one of the main limitations in single-molecule fluorescence (SMF) and super-resolution imaging. An attractive strategy to increase the photostability of organic fluorophores relies on their coupling to photostabilizers, e.g., triplet excited state quenchers, rendering self-healing dyes. Herein we report the self-healing properties of *tris*NTA-Alexa647 fluorophores (NTA, *N*-nitrilotriacetic acid). Primarily designed to specifically label biomolecules containing an oligohistidine tag, we hypothesized that the increased effective concentration of Ni(II) triplet state quenchers would lead to their improved photostability. We evaluated photon output, survival time, and photon count rate of different Alexa647-labeled *tris*NTA constructs differing in the length and rigidity of the fluorophore-*tris*NTA linker. Maximum photon output enhancements of 25-fold versus Alexa647-DNA were recorded for a short tetraproline linker, superseding the solution based photostabilization by Ni(II). Steady-state and time-resolved studies illustrate that *tris*NTA self-healing role is associated with a dynamic excited triplet state quenching by Ni(II). Here improved photophysical/photochemical properties require for a judicious choice of linker length and rigidity, and in turn a balance between rapid dynamic triplet excited state quenching versus dynamic/static singlet excited state quenching. *Tris*NTA fluorophores offer superior properties for SMF allowing specific labeling and increased photostability, making them ideal candidates for extended single-molecule imaging techniques.

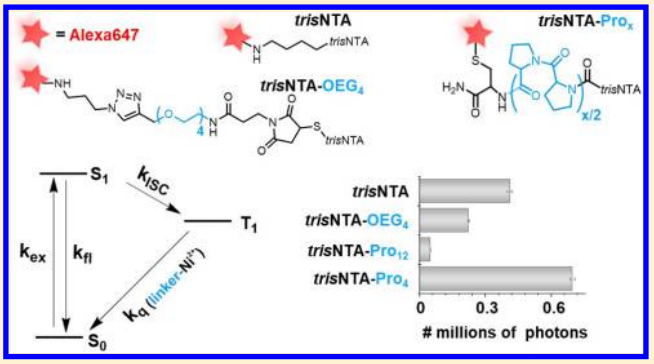

INTRODUCTION

The photostability of fluorophores plays a crucial role in single-molecule fluorescence (SMF) imaging and super-resolution imaging.[1,2] Photostability is typically improved using solution additives/photostabilizers that readily quench transient intermediates involved in photodegradation pathways, such as the excited triplet states of the fluorophores or their reactive radical intermediates.[3] However, photostabilizers at micromolar to hundreds of millimolar concentrations are required to efficiently intercept these intermediates, thus having the potential to perturb/affect the system under investigation, including toxic side effects in cell applications.[4] An attractive alternative strategy, often termed as a "self-healing"[5] approach, involves a direct conjugation of the photostabilizer to the fluorophores of interest, increasing the effective concentration of the quencher.[6] Such intramolecular photostabilization was first proposed by Lüttke and colleagues, who attached triplet state quenchers[7] and singlet oxygen scavengers[8] to fluorophores used in dye lasers. Recently, intramolecular photostabilization was explored by Blanchard[9−12] and Cordes[5,13−16] groups, toward enhancing the photostability of fluorophores used for SMF imaging. Improved photostability has been shown for fluorophores tethered to cyclooctatetraene (COT), a triplet energy acceptor,[9−11] and Trolox (TX),[9,10,14−16] nitrobenzyl alcohol (NBA),[9,10] and nitrophenylalanine (NPA),[13,15,16] where the latter three are electron donor/acceptor moieties that operate via photoinduced electron transfer (PeT)-based triplet quenching.

Our previous work has shown that Ni(II) is an efficient photostabilizing agent for DNA-tethered single-molecule fluorophores including Cy5, Alexa Fluor 647 (from hereon Alexa647), ATTO647N, Cy3, ATTO532, and Alexa532. It provides for physical rather than chemical triplet state quenching yielding an increase in average photon output of up to 40-fold.[17,18] A major drawback of this system, however, lies in the potential toxicity of free Ni(II) ions in biological solutions and its potential lower affinity to peptides over DNA backbones. Parallel work by some of us has shown that Ni(II) ions may be conjugated to fluorophores via *N*-nitrilotriacetic

Received: May 7, 2018
Published: August 7, 2018

DOI: 10.1021/jacs.8b04681
J. Am. Chem. Soc. XXXX, XXX, XXX−XXX

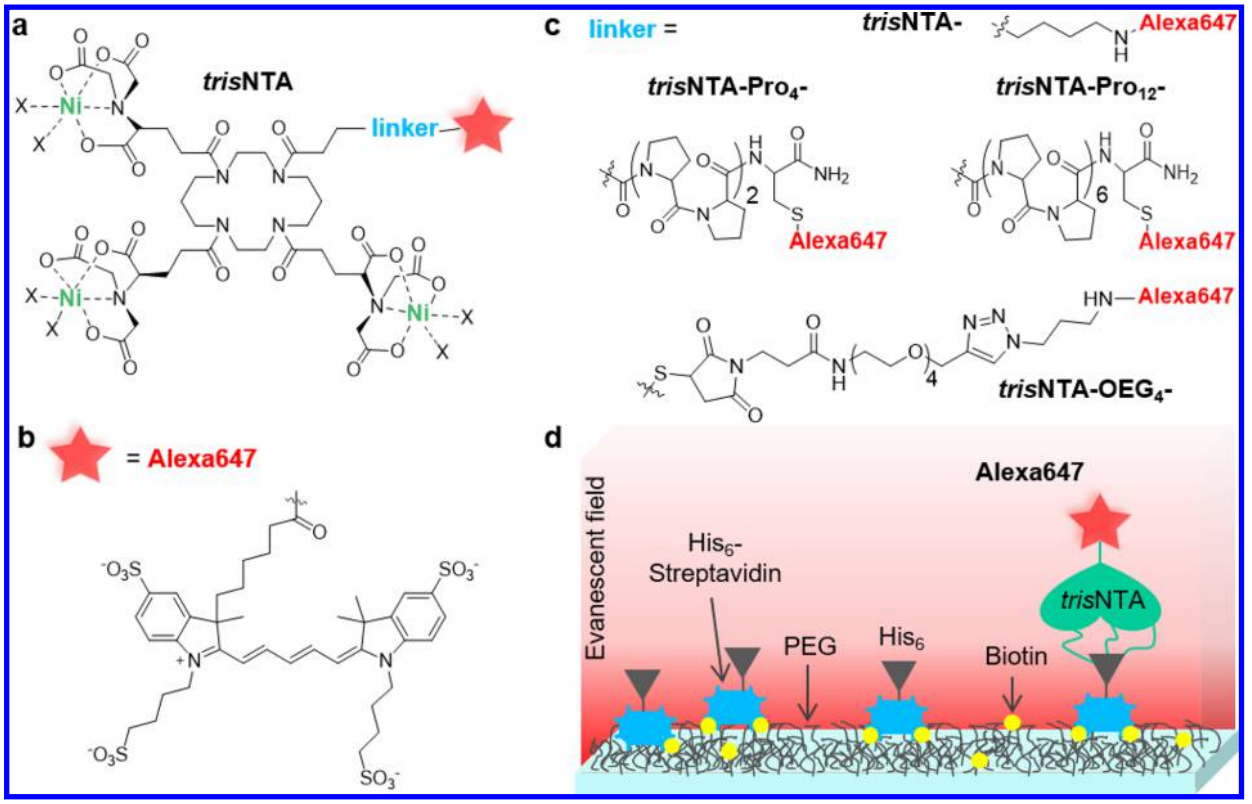

Figure 1. (a) Structure of *tris*NTA construct. (b) Structure of Alexa647. (c) Structure of the linkers used for *tris*NTA-Alexa647; *tris*NTA-Pro_{12}-Alexa647; *tris*NTA-Pro_4-Alexa647; and *tris*NTA-OEG_4-Alexa647 constructs. (d) Schematic illustration of the single-molecule experiment used to evaluate the photostability of *tris*NTA constructs.

acid (NTA) moieties allowing for specific, noncovalent yet kinetically stable ($k_{off} \sim 10^{-5}$ s^{-1}; $K_d \sim 0.1-10$ nM[19]) labeling of biomolecules containing the oligohistidine tag (His_{6-10} tag).[19−26] Efficient chelation of Ni(II) provided a handle and aborted any toxicity rendering *tris*NTA fluorophores suitable labels for a number of fluorescence imaging applications, including live-cell imaging studies.[21,25]

We reasoned that the complexation of three Ni(II) ions in the scaffold of *tris*NTA-fluorophores would impart an associated improvement in fluorophore photostability, provided Ni(II) proximity is sufficient to quench a fluorophore when in its triplet excited state, while sparing the much shorter-lived singlet excited state. *tris*NTA would serve, we posit, a dual role tagging the fluorophore to oligohistidine labeled biomolecules but also improving its photostability.

Herein we report SMF and ensemble steady-state and time-resolved studies on four Alexa647-labeled *tris*NTA constructs differing in the length and rigidity of the linker connecting both segments (Figure 1a−c). Our SMF results showed up to 25-fold increase in average number of photons collected for a construct bearing a short rigid tetraproline linker. The data illustrates that *tris*NTA protecting role is associated with dynamic quenching by Ni(II), where improved photophysical/photochemical properties for SMF experiments are obtained when dynamic, rather than static quenching operates.

Our mechanistic studies on the nature of the linker between connecting fluorophore and photostabilizer illustrate how length but also rigidity are key parameters to consider, where a balance between triplet excited state quenching versus singlet excited state quenching may control the ultimate yield of photon output when self-healing environments are exploited under high irradiation conditions encountered in SMF imaging. Overall, our results underscore that *tris*NTA fluorophores may be an optimal choice for single-molecule studies as the construct provides not only a handle to specifically tag proteins of interest but also a self-healing antifading property in the form of Ni(II) quenching of triplet excited states.

RESULTS AND DISCUSSION

To evaluate the photophysical properties of the various *tris*NTA-Alexa647 constructs (Figure 1a−c, Figure S1), we performed SMF studies using total internal reflection fluorescence (TIRF) microscopy. To specifically bind the *tris*NTA-Alexa647 constructs to the glass surface, a bottom-up self-assembly strategy was applied where we exploited the Ni(II)-*tris*NTA affinity for His_6-tagged proteins (Figure 1d). Here, polyethylene glycol (PEG) coated glass coverslips were prepared.[27−29] A small fraction (1%) of PEG polymers was biotinylated, which allowed us to specifically immobilize His_6-labeled streptavidin proteins on the surface. Surface bound His_6-streptavidin in turn enabled the specific immobilization of *tris*NTA-fluorophores via Ni(II)-*tris*NTA/His_6-Tag interactions. Control experiments without streptavidin, with streptavidin lacking His_6, or incubation with EDTA (a strong chelator for Ni(II) ions) confirmed the specific nature of this binding (Figure S2). Upon excitation with a 635 nm laser, images containing hundreds of single molecules were acquired on an EMCCD camera. The fluorescence intensities of single Alexa647 fluorophores were monitored over time in the presence of an oxygen scavenger to determine for each molecule the survival time, average intensity as well as the number of total photons collected before photobleaching

DOI: 10.1021/jacs.8b04681
J. Am. Chem. Soc. XXXX, XXX, XXX−XXX

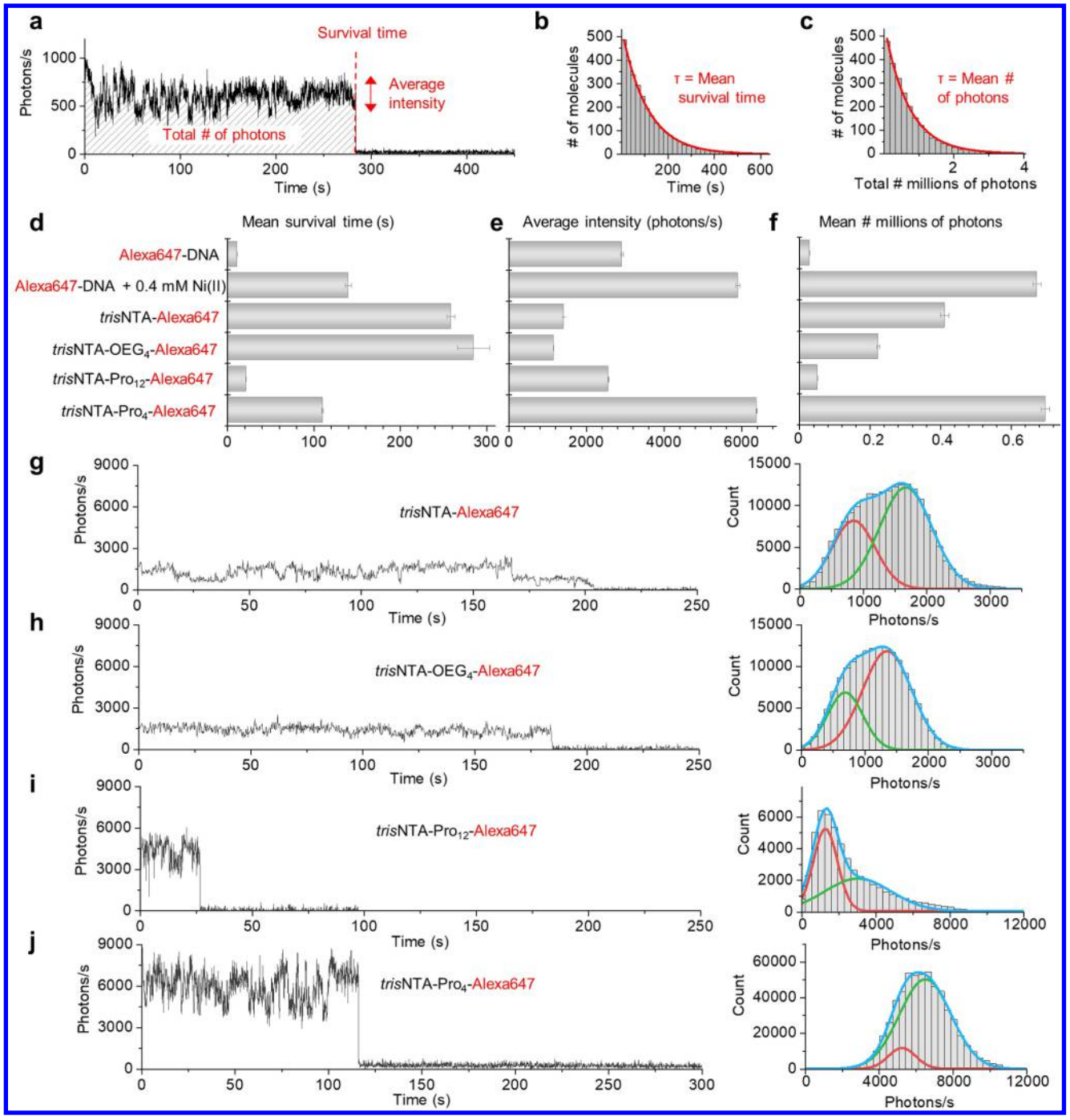

Figure 2. Characterization of different *tris*NTA-Alexa647 constructs in SMF studies. (a) Illustration of how survival time, total number of photons, and average intensity were obtained from SMF trajectories. (b) The mean survival time for each construct was obtained from the survival time histogram. (c) The mean number of photons collected for each construct was obtained from the histogram of total number of photons/molecule. Panels d, e, and f show the mean survival time, average count rate, and mean number of photons detected, respectively, for different *tris*NTA-Alexa647 constructs explored in this work. Panels g, h, i, and j show representative single-molecule fluorescence trajectories (100 ms/frame) and intensity distribution histograms obtained, respectively, for *tris*NTA-Alexa647, *tris*NTA-OEG$_4$-Alexa647, *tris*NTA-Pro$_{12}$-Alexa647, and *tris*NTA-Pro$_4$-Alexa647.

(Figure 2a and Table S1). The mean survival time (τ_s) and mean number of photons (τ_p) were next estimated by building the survival time and photon histograms and fitting them to single exponential decay functions (Figure 2b,c).

Figure 2d–f compares the mean survival times, average intensities, and mean number of photons detected for different *tris*NTA Alexa647 constructs. We first evaluated the most common construct (*tris*NTA-Alexa647), in which the fluorophore and the *tris*NTA moiety are connected by a short alkyl chain (Figure 1c). We compared the photostability of this construct to that of Alexa647 when attached to a DNA duplex and immobilized on the glass surface via biotin–streptavidin interactions.[17] The mean photon output of *tris*NTA-Alexa647 was 15-fold higher than the photon output of Alexa647-DNA duplex in the absence of any photostabilizer (Figure 2f, Table

DOI: 10.1021/jacs.8b04681
J. Am. Chem. Soc. XXXX, XXX, XXX–XXX

S1), illustrating that the *tris*NTA moiety rendered an improved photostability for Alexa647 under SMF imaging conditions.

In order to evaluate the improvement in photostability for the self-healing *tris*NTA-Alexa647 construct versus the solution-based photostabilization by free Ni(II), we compared its total photon output to that of Alexa647-DNA duplex in the presence of 0.4 mM Ni(II) as a solution additive. We were initially surprised that the self-healing approach in the *tris*NTA construct was less efficient compared to the solution-based photostabilization. A 24-fold increase in photostability was achieved in the latter compared to a 15-fold in the former (Figure 2f, Table S1).[18] Moreover, the brightness (average intensity) of the *tris*NTA-Alexa647 construct was ~4-fold lower when compared to that of Alexa647-DNA duplex in the presence of 0.4 mM Ni(II) (Figure 2e).

We hypothesized that the lower photostability and brightness of *tris*NTA-Alexa647 is associated with fluorescence (singlet excited state) quenching of Alexa647 by three Ni(II) ions present in too close proximity to the fluorophore. Our previous mechanistic studies on fluorophores bound to DNA duplexes[17,18] have shown that the photostabilization of fluorophores under low Ni(II) concentrations (0.1−1.0 mM) can be achieved with minimal fluorescence quenching. Under the high duty-cycle conditions of SMF imaging, a small loss of photons due to the quenching of singlet excited states is amply compensated by shortening the lifetime of/eliminating non-emissive long-lived triplet excited states. Further, we have shown that under these conditions the fluorophore and the Ni(II) ions encounter in primarily dynamic fashion leading to almost no static fluorescence quenching. On the other hand, the three Ni(II) ions present in close proximity to the fluorophore in *tris*NTA-Alexa647 could potentially result in a very rapid dynamic, or even static, singlet excited state quenching. The latter would not only reduce the quantum yield of the fluorophore leading to its dimmer signal in a SMF imaging experiment, but could also potentially introduce an additional photobleaching pathway. Thus, a balance between minimal (and dynamic rather than static) singlet excited state quenching and optimal triplet excited state quenching is essential.

To measure the extent of static and dynamic fluorescence quenching in the *tris*NTA-Alexa647 construct we next performed steady-state and time-resolved fluorescence studies. The emission spectrum and fluorescence lifetime of *tris*NTA-Alexa647 were analyzed before and after incubating with EDTA. As shown in Figure 3 (also Table 1), the enhancement in fluorescence intensity ($I_0/I_{Ni(II)}$) upon incubating with EDTA allowed us to determine the overall extent of singlet state quenching by Ni(II) (both static and dynamic). In turn, the enhancement in fluorescence lifetime ($\tau_0/\tau_{Ni(II)}$) allowed us to estimate the fraction of singlet state quenching by Ni(II) associated with dynamic quenching. More than 6-fold fluorescence quenching (primarily static) was measured for *tris*NTA-Alexa647 consistent with its lower brightness and photostability in SMF studies when compared to Alexa647-DNA duplex. In fact, a pronounced fluorescence quenching was also observed in our preliminary studies with other *tris*NTA-fluorophore constructs bearing Cy3, Cy5, and ATTO647N (Figure S3). Static quenching has led to their lower photostability in SMF studies in relation to the solution-based photostabilization with Ni(II) ions when tagged to DNA.

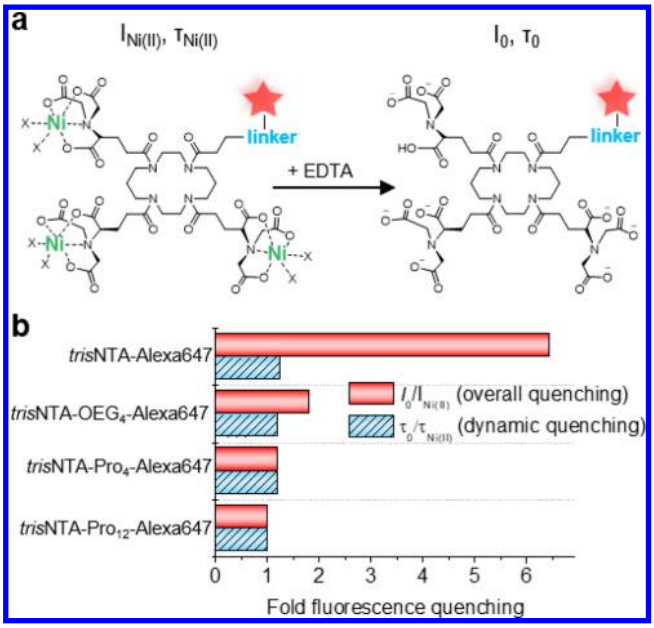

Figure 3. Evaluation of the extent of overall and dynamic fluorescence quenching in *tris*NTA-Alexa647 constructs. (a) Cartoon illustrating the experimental approach. Fluorescence intensities (integrated emission spectra) and fluorescence lifetimes were measured before ($I_{Ni(II)}$, $\tau_{Ni(II)}$) and after (I_0, τ_0) incubation with EDTA. (b) Extent of overall (red) and dynamic (blue) fluorescence quenching determined for different *tris*NTA-Alexa647 constructs.

Table 1. Average Intensity-Weighted Fluorescence Lifetimes of *tris*NTA-Alexa647 and Alexa647-DNA Constructs in the Absence and Presence of Ni(II) Ions Measured To Determine the Extent of Dynamic Fluorescence Quenching[a]

	average fluorescence lifetime[b] (ns)	
	$\tau_{Ni(II)}$	τ_0
construct	before EDTA	after EDTA
*tris*NTA-Alexa647	0.80	1.00
*tris*NTA-Pro$_{12}$-Alexa647	1.24	1.23
*tris*NTA-OEG$_4$-Alexa647	0.69	0.83
*tris*NTA-OEG$_4$-Alexa647 in 50% glycerol	1.15	1.46
*tris*NTA-Pro$_4$-Alexa647	1.03	1.25
*tris*NTA-Pro$_4$-Alexa647 in 50% glycerol	1.45	1.68
	$\tau_{Ni(II)}$	τ_0
	+0.4 mM Ni(II)	no Ni(II)
Alexa-647 DNA duplex	1.02	1.23

[a]For different *tris*NTA-Alexa647 constructs, the fluorescence lifetimes in the absence of Ni(II) were obtained by incubating with 5 mM EDTA. [b]Intensity-weighted average lifetimes. Values were obtained by fitting the fluorescence intensity decay curves to biexponential decay functions and using next the two preexponential values and associated decay lifetimes in the calculation. For biexponential fitting parameters including χ^2 values, see Table S2.

A structure that minimized fluorescence quenching while optimizing the dynamic encounter between the fluorophore and the *tris*NTA group, we reasoned, would render self-healing *tris*NTA constructs characterized by improved fluorophore photostability. To evaluate this hypothesis, we examined the photophysical properties of *tris*NTA-dyes containing longer flexible and rigid linkers (Figure 1c). Previous studies have

DOI: 10.1021/jacs.8b04681
J. Am. Chem. Soc. XXXX, XXX, XXX−XXX

demonstrated that introducing a linker (such as oligoethylene glycol (OEG_x) or oligoproline helix (Pro_x) between the fluorophore and the *tris*NTA group can help minimize the fluorescence quenching by Ni(II).[22,23]

We first tested the photophysical properties of *tris*NTA-OEG_4-Alexa647 with a longer flexible linker between the fluorophore and *tris*NTA moiety. Ensemble fluorescence quenching studies confirmed that introducing the OEG_4 linker helped to reduce the fluorescence quenching by Ni(II) from ~6.4-fold in *tris*NTA-Alexa647 to 1.8-fold in *tris*NTA-OEG_4-Alexa647 (Figure 3b). Nevertheless, single *tris*NTA-OEG_4-Alexa647 molecules still appeared dim in single-molecule studies (Figure 2b,e), leading to only slight improvement in mean number of total photons detected in SMF studies. Given the shorter average fluorescence lifetime of *tris*NTA-OEG_4-Alexa647 in the absence of Ni(II) ions (0.83 ns, Table 1) when compared to *tris*NTA-Alexa647 also in the absence of Ni(II) ions (1.00 ns, Table 1), we postulate that *tris*NTA-OEG_4-Alexa647 must exhibit an additional nonradiative decay pathway. Cyanine dyes, such as Cy3, Cy5, and Alexa647, exhibit an efficient nonradiative relaxation due to *trans*−*cis* photoisomerization, rendering their emission quantum yield extremely sensitive to local molecular environment and viscosity.[30] We suggest that the lower brightness of the *tris*NTA-OEG_4-Alexa647 construct arises from the lower rigidity of the fluorophore surrounding environment. This hypothesis is also consistent with an almost 2-fold increase in the fluorescence lifetime of *tris*NTA-OEG_4-Alexa647 when measured in a 50/50 (v/v) water/glycerol solution (Table 1).

To explore whether the brightness of Alexa647 could be preserved by replacing the OEG_4 linker with a more rigid one we evaluated the photophysical properties of *tris*NTA-Pro_{12}-Alexa647 and *tris*NTA-Pro_4-Alexa647 containing rigid Pro_{12} and Pro_4 helices as linkers, respectively (Figure 1c). As demonstrated by ensemble fluorescence studies (Figure 3 and Table 1), the introduction of a longer helix in *tris*NTA-Pro_{12}-Alexa647 construct eliminated the fluorescence quenching by Ni(II) ions. Here the same fluorescence lifetimes were obtained before and after Ni(II) removal from the construct (1.24 and 1.25 ns, respectively). This resulted in brighter signal from single fluorophores in SMF studies (Figure 2e,i). Nevertheless, the average survival time of *tris*NTA-Pro_{12}-Alexa647 was much shorter than the one observed for *tris*NTA-Alexa647 or *tris*NTA-OEG_4-Alexa647 constructs (Figure 2d), suggesting that the longer Pro_{12} helix prevented the desired dynamic collisions between Alexa647 and Ni(II) to occur in a timely fashion to efficiently quench the triplet excited state of the dye. Fluorescence intensity autocorrelations[31,32] of individual immobilized *tris*NTA-Pro_{12}-Alexa647 and *tris*NTA-Pro_4-Alexa647 showed that the triplet excited state was observable for the former, but not the latter construct. Thus, a contribution to the amplitude of the autocorrelation relaxation curve in the microsecond domain, consistent with the triplet excited state decay, was recorded for *tris*NTA-Pro_{12}-Alexa647 in the oxygen scavenger buffer, which is absent from the *tris*NTA-Pro_4-Alexa647 construct under similar conditions. For the Pro_4 construct rapid intramolecular deactivation of the triplet excited state prevents its observation within the time resolution of our intensity autocorrelation analysis, see Figure S4. Importantly, the contribution to the amplitude assigned to the triplet state is also absent for *tris*NTA-Pro_{12}-Alexa647 in an air equilibrated buffer lacking the oxygen scavenger.

Optimal photostabilization was thus achieved for *tris*NTA-Pro_4-Alexa647 with a short yet rigid Pro_4 linker. The extent of fluorescence quenching in *tris*NTA-Pro_4-Alexa647 was drastically minimized if compared to *tris*NTA-Alexa647 (Figure 3) while the triplet excited state was efficiently quenched (Figure S4). Single fluorophore molecules appeared very bright in single-molecule studies, allowing for detection of 6400 photons/s from single Alexa647 dye (Figure 2e,j). The longer fluorescence decay lifetimes of *tris*NTA-Pro_{12}-Alexa647 and *tris*NTA-Pro_4-Alexa647 in the absence of Ni(II) (1.23 and 1.25 ns, respectively) when compared to *tris*NTA-OEG_4-Alexa647 (0.83 ns) confirmed that nonradiative decay pathways in these constructs bearing the rigid polyproline helices are minimized and are comparable to Alexa647-DNA duplex (1.23 ns; Table 1). Consistent with this observation, the fluorescence lifetime of *tris*NTA-Pro_4-Alexa647 was less sensitive to increased viscosity (Table 1).

Importantly, the photostability of Alexa647 in the *tris*NTA-Pro_4-Alexa647 construct even slightly superseded the photostabilization that was previously obtained in the presence of Ni(II) as solution additive (Figure 2f). Overall, these results demonstrate that by a judicious choice of the linker length and rigidity one can minimize fluorescence quenching and nonradiative decay pathways while still preserving the dynamic triplet state quenching pathway, achieving photostabilization via self-healing strategy that meets or even supersedes the solution-based approach.

To further assess the potential of the *tris*NTA-dyes for single-molecule imaging, we also closely examined the SMF trajectories obtained for each construct. Photostability is a crucial parameter to almost all single-molecule imaging applications, however, for some SMF techniques, e.g., single-molecule Förster resonance energy transfer (SM-FRET) or protein-induced fluorescence enhancement (SM-PIFE),[33,34] a stable fluorescent signal is also of paramount importance. As illustrated by selected SMF trajectories (see Figure 2d-g), fluctuating intensity behavior was observed in all *tris*NTA-Alexa647 constructs. Two different intensity populations were distinguished in SMF trajectories and in their related intensity histograms (Figure 2g-j). The fluctuating emission behavior of *tris*NTA-fluorophores observed in their SMF intensity-time trajectories spanned the second-time scales. Conformational changes occurring within the *tris*NTA construct or the attached streptavidin could not account for this fluctuation, as these processes typically occur on much shorter time scales. We suggest that different intensity states and fluctuating emission properties could be attributed to the reversible *mono*NTA-histidine interaction (k_{off} = 1.8 s^{-1}, K_d = 14 μM).[19,35] While the overall binding of *tris*NTA to oligohistidine tag is extremely stable, the transient binding and dissociation of single NTA group to oligohistidine could potentially lead to different extents of quenching by Ni(II) ions (e.g., Ni(II) getting closer to the fluorophore upon dissociation or change in quenching efficiency of Ni(II) due to the change of its ligands). This fluctuating emission behavior would hinder the use of *tris*NTA-fluorophores in SMF studies that rely on quantitative changes in signal intensity, such as SM-FRET or SM-PIFE. On the other hand, high photostability and photon output of *tris*NTA-constructs, such as *tris*NTA-Pro_4-Alexa647, would make them ideal candidates for extended single-molecule imaging techniques, such as single-particle tracking.

The self-healing approach by conjugation to *tris*NTA moieties is an attractive strategy as it allows to position three

DOI: 10.1021/jacs.8b04681
J. Am. Chem. Soc. XXXX, XXX, XXX−XXX

triplet state quenchers, e.g., Ni(II) ions, in close proximity to a fluorophore, maximizing the potential for triplet excited state quenching efficiency. Different from redox-based triplet state quenchers, Ni(II) quenches triplet excited states via a photophysical mechanism,[17] therefore avoiding the formation of potential radical intermediates, and chemical damage to the quencher (healing) moiety as it may be sometimes observed under self-healing conditions relying on ROXS mechanisms.[14] What makes *tris*NTA-fluorophores most attractive is that the photostability comes associated with highly specific targeting ability from the *tris*NTA group, allowing for robust, specific,[19,23] and photostable labeling of biomolecules of interest, targeted delivery[25] and minimal toxicity (as compared to free Ni(II) as photostabilizer) in live-cell imaging experiments.[21,25,36] As the trisNTA/His-tag interaction was successfully utilized in single-particle tracking[22] as well as single-molecule localization microscopy in living cells,[25,26] both techniques will synergistically profit by the improved photostability combined with the highly specific protein labeling.

CONCLUSION

In conclusion, SMF studies on *tris*NTA-Alexa647 constructs revealed that conjugation of fluorophores to three Ni(II) ions via NTA groups not only allows for the specific labeling of biomolecules of interests but also improves the photostability of the parent fluorophore. Our studies underscore the important role of the linker when designing efficient self-healing dyes containing triplet state quenchers that are also potential fluorescence quenchers. Here, we show that successful photostabilization of model Alexa647 fluorophore requires a minimization of unproductive singlet excited state quenching and nonradiative decay pathways and optimization of desired triplet excited state quenching pathway. This rational optimization of the linker in the *tris*NTA self-healing scaffold allowed us to demonstrate up to 25-fold improvement in photon output of Alexa647 dye. The advent of new Ni(II) chelators such as the recently developed *hexa*NTA,[36,37] while permitting tighter binding to the substrate of interest, will require an optimization of Pro_x linkers to satisfy a "Goldilocks zone" where efficient triplet excited state quenching takes place yet minimal fluorescence quenching occurs. Ultimately, we posit that the optimized constructs will permit kinetic profiling of His-tagged proteins as well as single-molecule super-resolution imaging in live, intact cells.

ASSOCIATED CONTENT

Supporting Information

The Supporting Information is available free of charge on the ACS Publications website at DOI: 10.1021/jacs.8b04681.

All the materials and methods including synthesis and characterization of new compounds (PDF)

AUTHOR INFORMATION

Corresponding Authors

*gonzalo.cosa@mcgill.ca
*tampe@em.uni-frankfurt.de

ORCID

Robert Tampé: 0000-0002-0403-2160
Gonzalo Cosa: 0000-0003-0064-1345

Present Address

§Department of Chemistry and Pharmacy, Ludwig-Maximilian University of Munich, Butenandt-Str. 5-11, 81377 Munich, Germany

Notes

The authors declare no competing financial interest.

ACKNOWLEDGMENTS

The German Research Foundation (SFB 902, SPP 1623, GRK 1986, SFB 807, and EXC 115 to R.T.) and the Volkswagen Foundation (Az. 91 067 to R.W. and R.T.) supported this work. G.C. is grateful to the Natural Science and Engineering Research Council of Canada (NSERC), the Fonds de Recherche du Quebec – Nature et Technologie (FQRNT), and the Canadian Foundation for Innovation (CFI) for funding. V.G. and Y.G. are thankful to the Drug Discovery and Training Program and NSERC CREATE Bionanomachines programs for postgraduate scholarships. V.G. is also thankful to Groupe de Recherche Axé sur la Structure des Protéines (GRASP) and Y.G. is also thankful to Vanier Canada, for postgraduate scholarships.

REFERENCES

(1) Ha, T.; Tinnefeld, P. *Annu. Rev. Phys. Chem.* **2012**, *63*, 595–617.
(2) Minoshima, M.; Kikuchi, K. *JBIC, J. Biol. Inorg. Chem.* **2017**, *22*, 639–652.
(3) Juette, M. F.; Terry, D. S.; Wasserman, M. R.; Zhou, Z.; Altman, R. B.; Zheng, Q.; Blanchard, S. C. *Curr. Opin. Chem. Biol.* **2014**, *20*, 103–111.
(4) Alejo, J. L.; Blanchard, S. C.; Andersen, O. S. *Biophys. J.* **2013**, *104*, 2410–2418.
(5) Tinnefeld, P.; Cordes, T. *Nat. Methods* **2012**, *9*, 426–427.
(6) Zheng, Q.; Juette, M. F.; Jockusch, S.; Wasserman, M. R.; Zhou, Z.; Altman, R. B.; Blanchard, S. C. *Chem. Soc. Rev.* **2014**, *43*, 1044–1056.
(7) Liphardt, B.; Liphardt, B.; Lüttke, W. *Opt. Commun.* **1981**, *38*, 207–210.
(8) Liphardt, B.; Liphardt, B.; Lüttke, W. *Opt. Commun.* **1983**, *48*, 129–133.
(9) Altman, R. B.; Terry, D. S.; Zhou, Z.; Zheng, Q.; Geggier, P.; Kolster, R. A.; Zhao, Y.; Javitch, J. A.; Warren, J. D.; Blanchard, S. C. *Nat. Methods* **2012**, *9*, 68–71.
(10) Altman, R. B.; Zheng, Q.; Zhou, Z.; Terry, D. S.; Warren, J. D.; Blanchard, S. C. *Nat. Methods* **2012**, *9*, 428–429.
(11) Zheng, Q.; Jockusch, S.; Rodriguez-Calero, G. G.; Zhou, Z.; Zhao, H.; Altman, R. B.; Abruna, H. D.; Blanchard, S. C. *Photochem. Photobiol. Sci.* **2016**, *15*, 196–203.
(12) Zheng, Q.; Jockusch, S.; Zhou, Z.; Altman, R. B.; Zhao, H.; Asher, W.; Holsey, M.; Mathiasen, S.; Geggier, P.; Javitch, J. A.; Blanchard, S. C. *Chem. Sci.* **2017**, *8*, 755–762.
(13) van der Velde, J. H. M.; Uusitalo, J. J.; Ugen, L.-J.; Warszawik, E. M.; Herrmann, A.; Marrink, S. J.; Cordes, T. *Faraday Discuss.* **2015**, *184*, 221–235.
(14) van der Velde, J. H. M.; Ploetz, E.; Hiermaier, M.; Oelerich, J.; de Vries, J. W.; Roelfes, G.; Cordes, T. *ChemPhysChem* **2013**, *14*, 4084–4093.
(15) van der Velde, J. H. M.; Oelerich, J.; Huang, J.; Smit, J. H.; Hiermaier, M.; Ploetz, E.; Herrmann, A.; Roelfes, G.; Cordes, T. *J. Phys. Chem. Lett.* **2014**, *5*, 3792–3798.
(16) van der Velde, J. H. M.; Oelerich, J.; Huang, J.; Smit, J. H.; Aminian Jazi, A.; Galiani, S.; Kolmakov, K.; Guoridis, G.; Eggeling, C.; Herrmann, A.; Roelfes, G.; Cordes, T. *Nat. Commun.* **2016**, *7*, 10144.
(17) Glembockyte, V.; Lincoln, R.; Cosa, G. *J. Am. Chem. Soc.* **2015**, *137*, 1116–1122.
(18) Glembockyte, V.; Lin, J.; Cosa, G. *J. Phys. Chem. B* **2016**, *120*, 11923–11929.

DOI: 10.1021/jacs.8b04681
J. Am. Chem. Soc. XXXX, XXX, XXX–XXX

(19) Tinazli, A.; Tang, J.; Valiokas, R.; Picuric, S.; Lata, S.; Piehler, J.; Liedberg, B.; Tampé, R. *Chem. - Eur. J.* **2005**, *11*, 5249−5259.
(20) Kapanidis, A. N.; Ebright, Y. W.; Ebright, R. H. *J. Am. Chem. Soc.* **2001**, *123*, 12123−12125.
(21) Wieneke, R.; Labòria, N.; Rajan, M.; Kollmannsperger, A.; Natale, F.; Cardoso, M. C.; Tampé, R. *J. Am. Chem. Soc.* **2014**, *136*, 13975−13978.
(22) Grunwald, C.; Schulze, K.; Giannone, G.; Cognet, L.; Lounis, B.; Choquet, D.; Tampé, R. *J. Am. Chem. Soc.* **2011**, *133*, 8090−8093.
(23) Lata, S.; Gavutis, M.; Tampé, R.; Piehler, J. *J. Am. Chem. Soc.* **2006**, *128*, 2365−2372.
(24) Zhao, C.; Hellman, L. M.; Zhan, X.; Bowman, W. S.; Whiteheart, S. W.; Fried, M. G. *Anal. Biochem.* **2010**, *399*, 237−245.
(25) Kollmannsperger, A.; Sharei, A.; Raulf, A.; Heilemann, M.; Langer, R.; Jensen, K. F.; Wieneke, R.; Tampé, R. *Nat. Commun.* **2016**, *7*, 10372.
(26) Wieneke, R.; Raulf, A.; Kollmannsperger, A.; Heilemann, M.; Tampé, R. *Angew. Chem., Int. Ed.* **2015**, *54*, 10216−10219.
(27) Godin, R.; Liu, H.-W.; Smith, L.; Cosa, G. *Langmuir* **2014**, *30*, 11138−11146.
(28) Karam, P.; Powdrill, M. H.; Liu, H.-W.; Vasquez, C.; Mah, W.; Bernatchez, J.; Götte, M.; Cosa, G. *J. Biol. Chem.* **2014**, *289*, 14399−14411.
(29) Marko, R. A.; Liu, H.-W.; Ablenas, C. J.; Ehteshami, M.; Götte, M.; Cosa, G. *J. Phys. Chem. B* **2013**, *117*, 4560−4567.
(30) Levitus, M.; Ranjit, S. *Q. Rev. Biophys.* **2011**, *44*, 123−51.
(31) Cosa, G.; Harbron, E. J.; Zeng, Y.; Liu, H.-W.; O'Connor, D. B.; Eta-Hosokawa, C.; Musier-Forsyth, K.; Barbara, P. F. *Biophys. J.* **2004**, *87*, 2759−2767.
(32) Cosa, G.; Zeng, Y.; Liu, H.-W.; Landes, C. F.; Makarov, D. E.; Musier-Forsyth, K.; Barbara, P. F. *J. Phys. Chem. B* **2006**, *110*, 2419−2426.
(33) Joo, C.; Balci, H.; Ishitsuka, Y.; Buranachai, C.; Ha, T. *Annu. Rev. Biochem.* **2008**, *77*, 51−76.
(34) Hwang, H.; Kim, H.; Myong, S. *Proc. Natl. Acad. Sci. U. S. A.* **2011**, *108*, 7414−7418.
(35) Dorn, I. T.; Neumaier, K. R.; Tampé, R. *J. Am. Chem. Soc.* **1998**, *120*, 2753−2763.
(36) Gatterdam, K.; Joest, E. F.; Dietz, M. S.; Heilemann, M.; Tampé, R. *Angew. Chem., Int. Ed.* **2018**, *57*, 5620−5625.
(37) Gatterdam, K.; Joest, E. F.; Gatterdam, V.; Tampé, R. The Scaffold Design of Trivalent Chelator Heads Dictates Affinity and Stability for Labeling His-tagged Proteins in vitro and in Cells. *Angew. Chem.*. **2018** DOI: 10.1002/ange.201802746.

DOI: 10.1021/jacs.8b04681
J. Am. Chem. Soc. XXXX, XXX, XXX−XXX